International Journal of Computational Methods
Vol. 17, No. 10 (2020) 2050008 (14 pages)

DOI: 10.1142/S0219876220500085

Hull Form Optimization Based on an NM+CFD Integrated Method for KCS

Aiqin Miao and Decheng Wan*

Computational Marine Hydrodynamics Lab (CMHL)
State Key Laboratory of Ocean Engineering
School of Naval Architecture, Ocean and Civil Engineering
Shanghai Jiao Tong University, Shanghai 200240, China
**dcwan@sjtu.edu.cn*

Received 11 December 2016
Revised 16 November 2019
Accepted 20 December 2019
Published 9 March 2020

This paper concerns development and illustration of a hydrodynamic optimization tool, OPTShip-SJTU, which contains four main components, i.e., hull form modifier, performance evaluator, surrogate model building, and optimizer module. It has been further developed by integrating a new method into the performance evaluator module, which combines the Neumann–Michell (NM) theory with computational fluid dynamics (CFD) technology, in order to reduce the high computational cost. To illustrate the practicality of further extension, OPTShip-SJTU was applied to optimize the hull form of KCS by simultaneously reducing drags at two speeds. A drag reduction was obtained by the optimal KCS of different hull forms. It turns out the presented method for ship optimization design is effective and reliable.

Keywords: Hull form optimization; drag; FFD; OPTShip-SJTU; naoe-FOAM-SJTU solver.

1. Introduction

Hull form optimization design is to obtain the new hull form(s) with the best hydrodynamic performances, through modifying the initial hull form locally or globally. It is a process in which to achieve the best hydrodynamics performance of a new ship directly drives ship design. With the development of computer technologies and computational fluid dynamics (CFD), hull form optimization design has raised the interest of researchers and designers, which is an inverse process absolutely different from the traditional ship design process almost depending on ship engineers' experience.

Recently, a rapidly increasing number of papers devoted to ship optimization design based on hydrodynamic performance have been yielded with the advantage of optimization techniques and high-performance computer (HPC), resulting in the

*Corresponding author.

huge development of ship design [Peri and Campana (2003); Tahara *et al.* (2011); Yang *et al.* (2014); Lee *et al.* (2014); Zhang and Miao (2015); Zhang *et al.* (2015)]. Most papers are concerned about the resistance performance optimization of a ship, where one of the most significant steps is the evaluation of the resistance. It is mainly divided into two methods, potential theory and CFD. Zhao *et al.* [2015] optimized wave resistance of Wigley based on Michell theory. Zhang and Zhang [2015] combined Rankine Method for wave resistance evaluation with 1957 ITTC formula for viscous resistance evaluation to approximate total resistance of S60 and made a reduction of 4.5% for total resistance by modifying the S60 hull form. Huang *et al.* [2016] reduced the total drag coefficient of a cargo ship approximately using NM theory for C_w evaluation and ITTC formula for C_f evaluation. Vasudev *et al.* [2014] optimized and designed AUVs using CFD for C_v by Shipflow software and made a drag reduction but spent a lot of time on the optimization process.

Potential theory is simple to realize by program and quick to evaluate the resistance, while it is the approximate method, it does not consider viscosity of water. CFD is a quite high-precision method of resistance evaluation, while it greatly increases the computational cost and time. Hull form optimization requires a good evaluation tool, which can evaluate the resistances of a series of new hull forms relatively with higher fidelity and lower computer cost. To sum up and further extend, a new idea is produced, which combines the NM potential theory with CFD method, called the NM+CFD integrated method here, to evaluate the resistance performance.

In this paper, KCS was chosen as the initial hull form to locally optimize its bow and stern, respectively, to minimize total resistance coefficients at two specific speeds. First, the design of experiment was used to select a reasonable optimal design space. Specifically, optimized Latin hypercube sampling (OLHS) method was applied here which satisfied the requirements of orthogonality and uniformity of samples to obtain different design variables, which represented different hull forms deformed by free form deformation (FFD) method. Next step was to evaluate their total resistances at two specific speeds, also called objective functions, where wave-making resistances were evaluated by NM theory and viscous resistances were evaluated by CFD-based naoe-FOAM-SJTU solver. Through those above different sample hull forms, the surrogate models were built to describe the implicit unknown relationship between the design variables and multi-objective functions, which largely decreased the optimization difficulty and computational cost. Last but not least, a vital multi-objective optimization process was completed by NSGA-II, a series of optimal ship hulls obtained. The whole optimization frame can be seen in Fig. 1.

2. Hull Form Deformation

An effective and rational method for hull form deformation is indispensable and crucial in the hydrodynamic optimization of ship hull forms. One hull form should be quickly and reasonably transformed to another new one. As few deformation

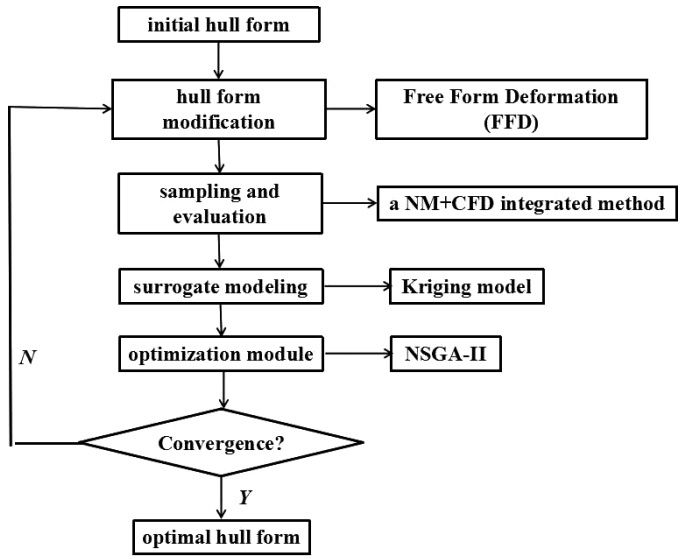

Fig. 1. The flow chart of the iterative optimization process.

parameters as possible can greatly accelerate the optimization process. Here FFD method is a good choice to modify hull form locally or globally. FFD method was first described by Sederberg and Parry [1986] and was based on an earlier technique by Barr [1984]. Its basic idea of this method is embedding a ship or the region of the ship to be deformed within a parallelepipedical three-dimensional (3D) lattice regularly subdivided. Then it can modify the surface shape of a ship by the following relationship:

$$X_{ffd} = \sum_{i=0}^{l} \sum_{j=0}^{m} \sum_{k=0}^{n} \mathrm{B}_{i,j}(s)\mathrm{B}_{j,k}(t)\mathrm{B}_{i,k}(u)Q'_{i,j,k}, \tag{1}$$

wherein $Q'_{i,j,k}$ is the coordinates of the control points on the lattice, while X_{ffd} is the coordinates of the points of the ship surface. B is Bernstein polynomial, l, m, and n are the numbers of the control points along the x-axis, y-axis, and z-axis direction, respectively. Through changing the number, direction, and displacement of the movable control points, the different ship surfaces can be easily obtained.

An application of FFD method to modify a ship bow is shown in Fig. 2. The surface to be deformed is wrapped by a parallelepiped lattice. There are two kinds of control points on the lattice, the movable control points (purple spheres) and fixed control points (yellow spheres). A different shape of the ship bow can be easily obtained due to the lateral displacement of the movable control points. In this paper, FFD method is applied to locally modify the bulb bow and the stern of KCS, respectively.

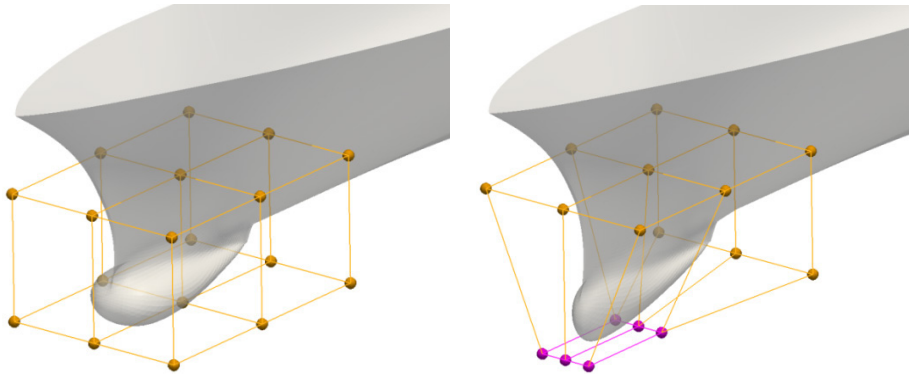

(a) Initial (b) Modified

Fig. 2. An application of FFD method to modify the ship bow (Left: the initial ship (a); right: the modified ship (b)).

3. Total Resistance Evaluation

The total resistance of ships can be solved according to two methods of division. One is according to the assumption of Froude through his experiments, Froude realized that the ship resistance had to be broken into two different parts: residuary resistance (mainly wave-making resistance) only related to Froude number (Fr) and frictional resistance only related to Reynolds number (Re). However, the influence of the two parts is ignored by using this method.

So in 1950s, Hughes proposed another method — 3D conversions, which was recommended as the standard conversion at ITTC in 1978. Through this conversion, total resistance (R_t) is broken into two new parts: wave-making resistance (R_w) related to Froude number and the viscous resistance (R_v) (the sum of the viscous pressure resistance and friction resistance) related to Reynolds number.

$$R_t = R_w + R_v. \tag{2}$$

In this paper, the above standard conversion is chosen to predict the total resistance, wave-making resistance calculated by NM theory and viscous resistance calculated by simulating the flow field around the double ship model based on RANS, which is abbreviated as the NM+CFD integrated evaluation. Noblesse *et al.* [2013] presented an efficient potential theory, Neumann–Michell (NM) theory, which provides more accurate prediction of wave-making resistance and wave profiles than the Hogner slender-ship approximation, with no appreciable increase in computational cost. Besides, there are lots of research about comparison of experimental results of wave-making resistance with numerical predictions obtained by the NM theory for the Wigley hull, the S60, and DTMB 5415 model [Huang *et al.* (2013); Yang *et al.* (2007)]. A RANS-based CFD solver naoe-FOAM-SJTU, which is developed under the framework of the open source code, OpenFOAM, and has been validated in prediction of many ships' resistance [Shen *et al.* (2011)].

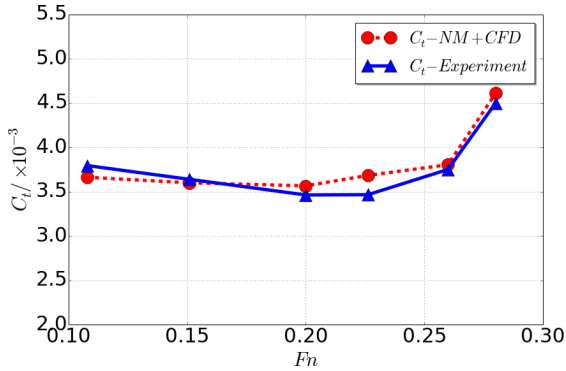

Fig. 3. Comparison of the total resistance coefficient of KCS predicted by the present method and experiment data.

The validation study for the NM+CFD integrated method was carried out before the optimization. For KCS, the comparison of the results calculated by the NM+CFD integrated method and experimental data are shown in Fig. 3.

From the above figure, the numerical results for KCS based on the NM+CFD integrated method agree with the experimental results very well. The maximum error is 2.45%, less than 3%. It turns out the present method can be used to predict the resistance. It is worth mentioning that this method can greatly reduce the computational time. First, wave-making resistance for a ship based on NM theory can be completed in a PC within seconds. In addition, the double ship model is applied on the calculation process, instead of a ship model with free surface, that is to say, the flow for simulation is transformed from two-phase flow to one-phase flow. For one case of a ship's resistance prediction, the double ship model simulation is twice as fast as the ship with free surface. These two key points are very beneficial to ship optimization design.

4. Kriging-Based Surrogate Model

To accelerate the hull form optimization process, a Kriging-based surrogate model is used to approximate the relationship between the design variables (input) and the objective functions (output). The details of Kriging-based surrogate model can be found in Kim *et al.* [2011]. There are four main steps to build a surrogate model in the ship hull form optimization for reduced resistance coefficients.

The design of experiments (DOE) is a strategy for choosing sample points in the design space. There are a lot of DOE methods in the literature, such as factorial design, Latin hypercube sampling (LHS), OLHS. In this work, OLHS method is adopted to allocate the sample points in the design space. Next, the candidate hull forms are produced using the surface modification tool from the chosen sample points, and their resistance performances (multi-objective functions) are then evaluated through an NM+CFD integrated method mentioned above.

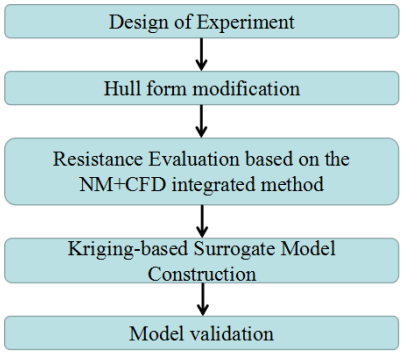

Fig. 4. Flowchart of the Kriging-based surrogate model construction.

With the constructed Kriging surrogate model, the cross validation [Jones *et al.* (1998)] is performed to examine the accuracy of the model. The basic idea of the cross validation is to leave out one sample point, and then predict it based on the surrogate model built by the remaining sample points. The difference between the true objective function value and the predicted value at this point is calculated. If the difference is small enough, the model is valid. Otherwise, more sample points will be needed, and then the Kriging surrogate model will be needed to rebuilt by iterating the steps shown in Fig. 4.

5. The Definition of Multi-Objective Optimization

A multi-objective optimization problem is a problem of multiple criteria decision making, that is concerned with mathematical optimization problems involving more than one objective function to be optimized simultaneously. Multi-objective optimization problem has been applied in many fields of science, including engineering, economics, and logistics where optimal decisions need to be taken in the presence of trade-offs between two or more conflicting objectives.

In mathematical terms, a multi-objective optimization problem can be formulated as

$$\begin{aligned} &\min(f_1(x), f_2(x), \ldots, f_k(x)), \quad k \geq 2 \\ &\text{s.t.} \quad x \in \mathrm{X} \end{aligned}, \tag{3}$$

where the integer k is the number of objectives and the set x is the feasible region.

In the ship industry, there is still a problem about the trade-offs between each performance of a new ship during the ship design process. The following content will clearly describe a complete multi-objective optimization of ship design.

6. The Establishment of the Optimization Problem

For an entire optimization problem to be solved, the following basic items must be specified in detail: (1) an initial hull form to be optimized and the region(s) to be

modified; (2) the objective functions to be minimized and the design variables to be used; (3) the constraints to be defined. All of these items will be described in terms of the ship optimization presented by this paper.

6.1. *Initial hull form*

The initial hull form is the KRISO 3600TEU container ship model (KCS), which was conceived to provide data for both explication of flow physics and CFD validation for a modern container ship with bulb bow and stern. There is a large experimental database for KCS due to an international collaborative study on experimental/numerical uncertainty assessment between National Maritime Research Institute (NMRI), Maritime and Ocean Engineering Research Institute (MOERI), and Schiffbau-Versuchsanstalt Potsdam GmbH (SVA) [Lee *et al.* (2003)]. The geometry of the initial model is presented in Fig. 5 and the principal dimensions of KCS in Table 1.

6.2. *Multi-objective functions and design variables*

The multi-objective functions to be minimized were the total resistance coefficients of KCS sailing in calm water at two speeds of Fr = 0.2, Fr = 0.26 (the design speed). This condition corresponds to using a reference length of 7.36 m, that is the length of the ship's model used in the experimental validation.

$$C_{\mathrm{t}} = C_{\mathrm{w}} + C_{\mathrm{v}}, \tag{4}$$

$$C_{\mathrm{w}} = \frac{R_w}{0.5\rho U^2 S}, \tag{5}$$

$$C_{\mathrm{v}} = \frac{R_v}{0.5\rho U^2 S}. \tag{6}$$

The deformation region was only the foremost part of the ship ($x = 3.45 \sim 3.99$ m) and the stern of the ship ($x = -3.44 \sim -0.44$ m), with the origin of coordinates at the midship in Fig. 6. As explained in the introduction, this is the typical redesign

Fig. 5. The geometry of KCS.

Table 1. The principal dimensions of KCS.

Principal dimensions	Full-scale ship	Ship model
Length between perpendiculars L_{pp} (m)	230	7.28
Length of waterlines L_{wl} (m)	232.5	7.36
Breadth molded B (m)	32.2	1.019
Depth molded D (m)	19	0.6013
Draught T (m)	10.8	0.3418
Block coefficient C_b	0.651	0.651

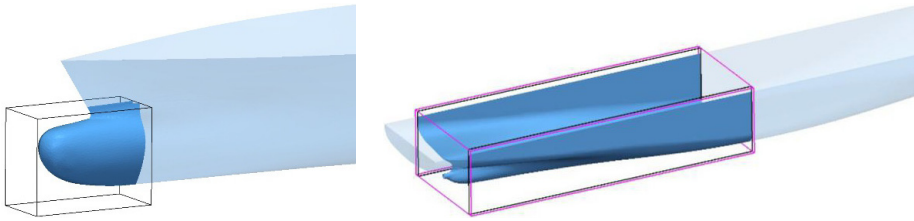

Fig. 6. The modification regions by FFD method.

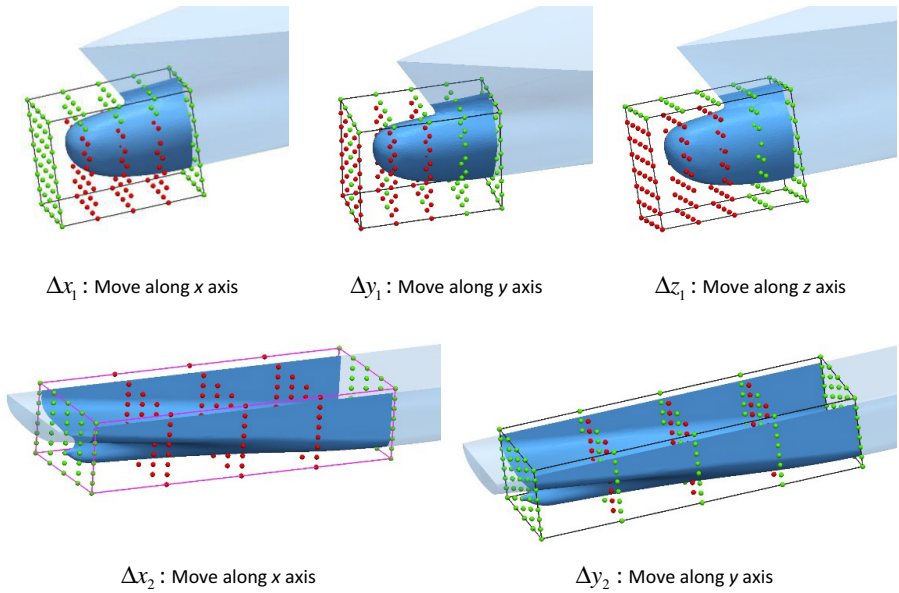

Fig. 7. The movement direction of some control points using by FFD method.

problem of some part of an existing complex system, a necessity which often arises in real industrial applications. At the stern of the ship, two control lattices were used in order to modify the origin shape of the stern to any practical new one within the fixed ship width. In Fig. 7, some certain movable control points and the other fixed control points are clearly grouped into two kinds of colors, red and green. As we can see, there are five design variables, Δx_1 (displacement of control points in x direction in the fore part), Δy_1 (displacement of control points in y direction in the fore part), Δz_1 (displacement of control points in z direction in the fore part), Δx_2 (displacement of control points in x direction in the aft part), and Δy_2 (displacement of control points in y direction in the aft part).

6.3. *The constraints*

Some geometric constraints were imposed on the design variables. The optimization problem presented here kept the main dimensions (L_{pp}, B, and D) of every new

Table 2. Definition of the optimization problem.

Type	Definition	Note
Initial hull	The KRISO 3600TEU container ship model (KCS)	
Objective functions	$f^1_{\text{obj}} = C_\text{t} = C_\text{w} + C_\text{v}$, at Fr = 0.2	Bare hull
	$f^2_{\text{obj}} = C_\text{t} = C_\text{w} + C_\text{v}$, at Fr = 0.26	Aim is to search for hull forms with potential drag reduction at given speeds
Design variables		
Δx_1 (Variable 1)	[−0.0736, 0.0736]	Displacement in x direction in the fore-part region
Δy_1 (Variable 2)	[−0.0368, 0.0368]	Displacement in y direction in the fore-part region
Δz_1 (Variable 3)	[−0.04784, 0.04784]	Displacement in z direction in the fore-part region
Δx_2 (Variable 4)	[−0.05152, 0.05152]	Displacement in x direction in the aft-part region
Δy_2 (Variable 5)	[−0.0736, 0.08832]	Displacement in y direction in the aft-part region
Geometric constraints		
Main dimensions	L_{pp}, D, and B are fixed	
Displacement (∇)	Maximum variation ±1%	
Wetted surface area (S_{wet})	Maximum variation ±1%	
Experimental design	OLHS method	Generate 40 sample points
Approximation model	Kriging model	
Optimizer	NSGA-II	
Size of population	150	
Number of generations	300	

hull form fixed and their maximum variations of displacement and wetted surface area less than 1%.

All the settings of the presented KCS ship design optimization are listed in Table 2.

7. Numerical Results: The Optimal Design

Two Kriging-based surrogate models were, respectively, used to approximate the total resistance coefficients at two speeds in the optimization. Based on the OLHS method, 40 sample points for five design variables were generated to build the surrogate model. Then the corresponding values of multi-objective function, total resistance coefficients, were obtained using the NM+CFD integrated method. The cross validation for the two models were performed and the results are shown in Fig. 8.

In the cross validation, each sample point was evaluated from the Kriging-surrogate model that was constructed by the other 39 sample points. It can be observed from Fig. 8 that the estimated objective function values ($\text{C}^\text{E}_\text{t}$) given by

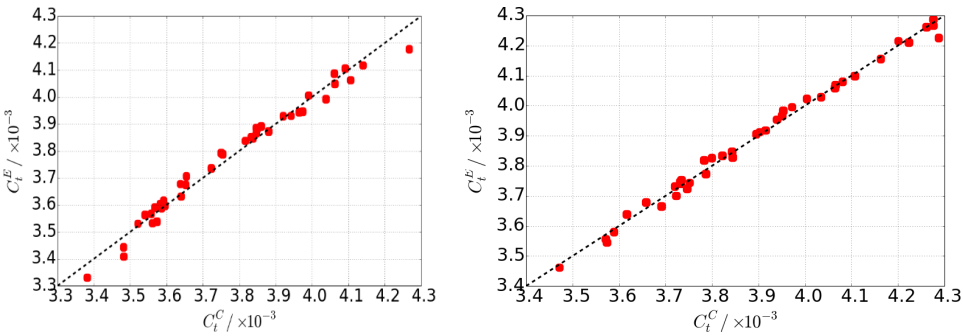

Fig. 8. Cross validations of the surrogate models about two objective functions.

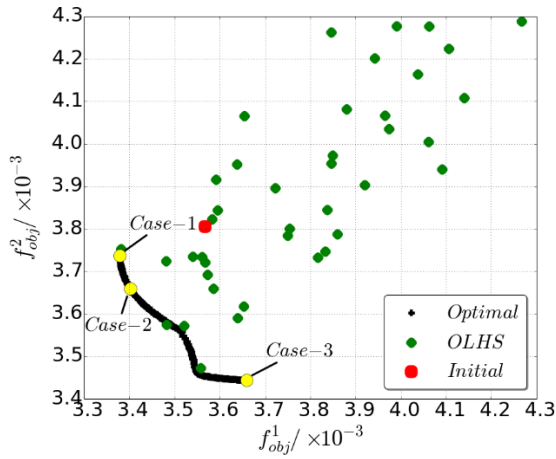

Fig. 9. Pareto optimal points and optimal cases in objective functions space.

the surrogate model show a good agreement with these (C_t^C) evaluated by the NM+CFD method directly for the objective functions.

The Pareto front by the NSGA-II algorithm is reported in Fig. 9, where each black point represents an optimal solution, each green point represents a sample point generated by OLHS method, and the red point represents the initial hull form while three typical cases are marked in yellow to be analyzed further.

Although the control modification regions are small, quite different configurations are readily yielded. All the Pareto optimal solutions representing different alternatives may be considered in the next design stage. Case-1, 2, and 3 are the optimal hull forms selected for further analysis in this paper. In the case-1 at its speed Fr = 0.2 and the case-3 at its Fr = 0.26, the total resistance coefficient decreases obviously, while in the case-2, it has decreased obviously at two speeds.

Their ship lines and the initial hull form lines shown in Fig. 10 differs from each other. Case-1 and 2 are narrower than the initial hull form especially at the aft-part

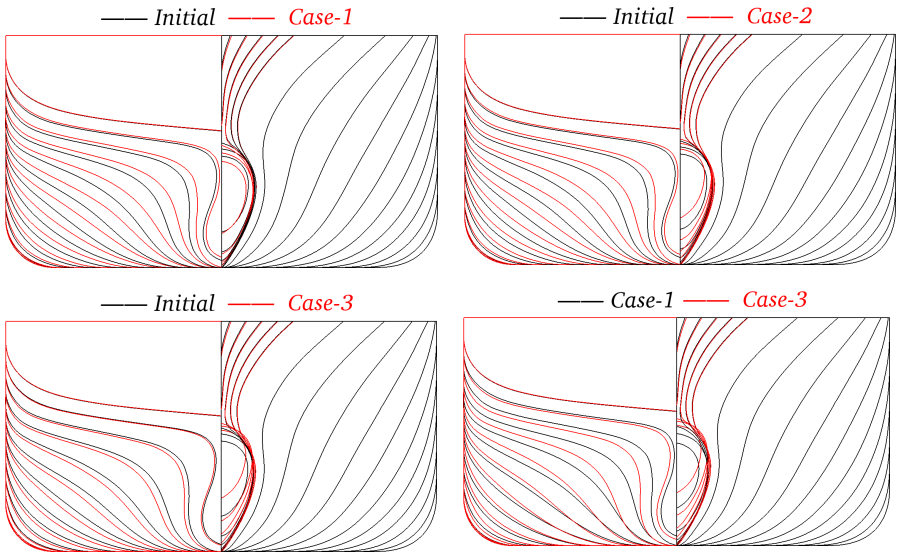

Fig. 10. Body plans between the initial hull form and the optimal hull forms.

Table 3. The prediction results for the initial and optimal hull forms based on the NM+CFD integrated method.

	C_t ($\times 10^{-3}$)		Reduction	
	Fr = 0.2	Fr = 0.26	Fr = 0.2 (%)	Fr = 0.26 (%)
Initial hull	3.567	3.805	—	—
Case-1	3.389	3.748	−4.99	−1.52
Case-2	3.396	3.644	−4.79	−4.24
Case-3	3.669	3.454	2.86	−9.24

of these two new ships, while Case-3 is slightly wider than the initial hull form. Case-2 and 3 are obviously upturned than the initial hull form at the bulb bow, while Case-1 has no obvious changes at the bulb bow.

Table 3 shows the reduction of the total resistance coefficient of the selected optimal hull forms at two speeds based on the NM+CFD integrated method. The total resistance coefficient of Case-1 has the most reduction at the speed of Fr = 0.2, while a little reduction at the speed of Fr = 0.26. The total resistance coefficient of Case-3 has the most reduction at the speed of Fr = 0.26, while a little increase at the speed of Fr = 0.2. Case-2 is a better choice than the two cases mentioned above, because both of its total resistance coefficients at the two speed decreases obviously. Figures 11 and 12 describe the pressure distribution at the bulb bow and the wake fields behind stern of the three cases and the initial ship. Case-2 and 3 bear a little smaller pressure than the initial hull form and the wake fields behind stern of the three ships have been improved than the initial ship.

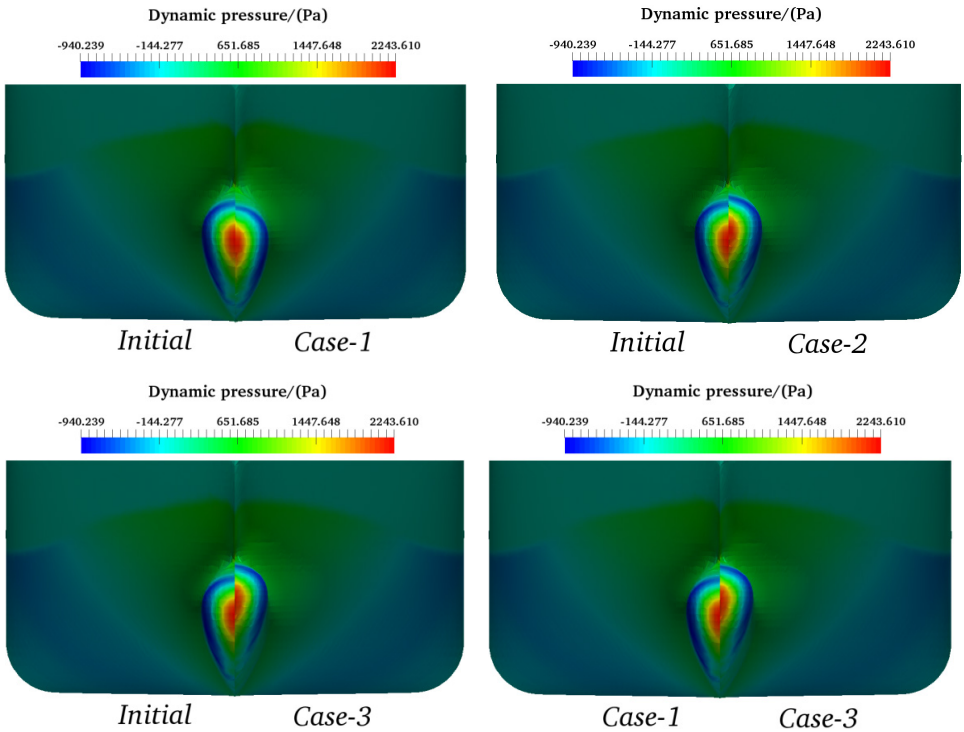

Fig. 11. Comparison of the pressure of the bulb bow between the initial hull form and the optimal hull forms.

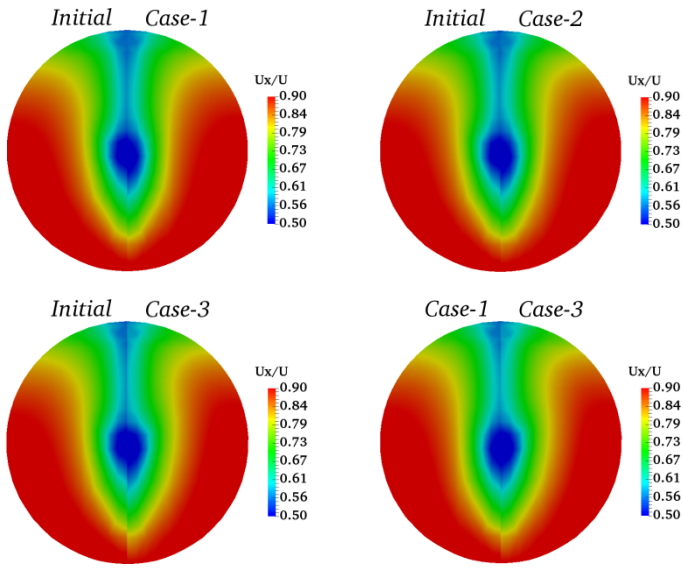

Fig. 12. Comparison of the pressure of the bulb bow between the initial hull form and the optimal hull forms.

8. Conclusions

(1) A numerical multi-objective optimization tool, OPTShip-SJTU, has been developed and applied in this work. The KCS ship was adopted as initial hull form, and the aim was to search for optimal hull forms with improved resistance performances at two given speeds (Fr = 0.20, 0.26).
(2) During the procedure of optimization, the regions of bulb bow and stern were deformed with FFD method. FFD method is sufficiently flexible to generate a series of realistic alternative hull forms with a few number of design variables involved.
(3) OPTShip-SJTU solver based on the integrated method of NM theory and Reynolds Average Navier Stokes (RANS) as the hydrodynamic performance evaluation module to predict the total resistance turns out to be applicable for a real optimization problem.
(4) Kriging-based surrogate models were built by the sample points generated by the OLHS method. The two models were reliable to predict the total resistance coefficients on the optimization process according to the results of cross validation.
(5) The results of OPTShip-SJTU solver should be further validated and verified by experimental data. After that, it can give a good guide to the ship hull form design.

Acknowledgments

This work is supported by the National Natural Science Foundation of China (51879159). The National Key Research and Development Program of China (2019YFB1704204, 2019YFC0312400), Chang Jiang Scholars Program (T2014099), Shanghai Excellent Academic Leaders Program (17XD1402300), and Innovative Special Project of Numerical Tank of Ministry of Industry and Information Technology of China (2016-23/09), to which the authors are most grateful.

References

Barr, A. H. [1984] "Global and local deformations of solid primitives," *Proc. 11th Annual Conf. Computer Graphics and Interactive Techniques*, Vol. 18, ACM, pp. 21–30.

Bagheri, H. and Ghassemi, H. [2014] "Genetic algorithm applied to optimization of the ship hull form with respect to seakeeping performance," *T. Famena.* **38**(3), 45–58.

Campana, E. F. *et al.* [2006] "Particle swarm optimization: Efficient globally convergent modifications," *III European Conf. Computational Mechanics*: *Solids*, *Structures and Coupled Problems in Engineering*, Lisbon, Portugal, pp. 1–18.

Huang, F., Yang, C. and Noblesse, F. [2013] "Numerical implementation and validation of the Neumann–Michell theory of ship waves," *J. Mech. B-Fluid.* **42**(6), 47–68.

Huang, F. *et al.* [2016] "A new improved artificial bee colony algorithm for ship hull form optimization," *Eng. Optim.* **48**(4), 672–686.

Jones, D. R., Schonlau, M. and Welch, W. J. [1998] "Efficient global optimization of expensive black-box functions," *J. Global Optim.* **13**(4) 455–492.

Kim, H. *et al.* [2011] "Hull form design exploration based on response surface method," *Proc. 21st Int. Offshore and Polar Engineering Conference*, Maui, Hawaii, USA, 816–825.

Lee, S. S. *et al.* [2014] "A study on optimization of ship hull form based on neuro-response surface method (NRSM)," *J. Mar. Sci. Tech-Taiw.* **22**(6), 746–753.

Lee, S. J. *et al.* [2003] "PIV velocity field measurements of flow around a KRISO 3600TEU container ship model," *J. Mar. Sci. Tech.* **8**(2), 76–87.

Noblesse, F., Huang, F. and Yang, C. [2013] "The Neumann–Michell theory of ship waves," *J. Eng. Math.* **79**(1), 51–71.

Peri, D. and Campana, E. F. [2003] "Multidisciplinary design optimization of a naval surface combatant," *J. Ship Res.* **47**(1), 1–12.

Sederberg, T. W. and Parry, S. R. [1986] "Free-form deformation of solid geometric models," *SIGGRAPH Comput. Graph.* **20**(4), 151–160.

Shen, Z. R. *et al.* [2011] "RANS simulations of benchmark ships based on open source code," *7th Int. Workshop on Ship Hydrodynamics* (*IWSH'2011*), Shanghai, China, pp. 76–82.

Tahara, Y. *et al.* [2011] "Single- and multi-objective design optimization of a fast multihull ship: Numerical and experimental results," *J. Mar. Sci. Tech.* **16**(4), 412–433.

Vasudev, K. L., Sharma, R. and Bhattacharyya, S. K. [2014] "A CAGD + CFD integrated optimization model for design of AUVs," *IEEE Oceans 2014 TAIPEI*, pp. 1–8.

Yang, C., Delhommeau, G. and Noblesse, F. [2007] "The Neumann–Kelvin and Neumann–Michell linear models of steady flow about a ship," *Int. Congress of the Int. Maritime Association of the Mediterranean Imam*, Taylor and Francis, London, pp. 129–136.

Yang, C. *et al.* [2014] "Hydrodynamic optimization of a triswach," *J. Hydrodyn.* **26**(6), 856–864.

Zhang, B. J. and Miao, A. Q. [2015] "The design of a hull form with the minimum total resistance," *J. Mar. Sci. Tech-Taiw.* **23**(5), 591–597.

Zhang, B. J. *et al.* [2015] "Research on design method of the full form ship with minimum thrust deduction factor," *China Ocean Eng.* **29**(2), 301–310.

Zhang, B. J. and Zhang, Z. X. [2015] "Research on theoretical optimization and experimental verification of minimum resistance hull form based on Rankine source method," *Int. J. Nav. Arch. Ocean.* **7**(5), 785–794.

Zhao, Y. *et al.* [2015] "Ship hull optimization based on wave resistance using wavelet method," *J. Hydrodyn.* **27**(2), 216–222.